

## Synthetic Methods

## Regioselective Hydroalkylation of Vinylarenes by Cooperative Cu and Ni Catalysis

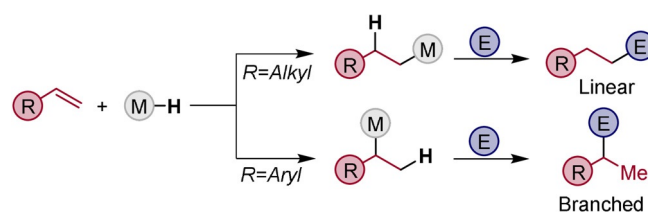
Anne K. Ravn, Martin B. Johansen, and Troels Skrydstrup\*

**Abstract:** Disclosed here is a dual copper and nickel catalytic system with a silyl hydride source for promoting the linear selective hydroalkylation of vinylarenes. This carbon–carbon bond-forming protocol is applied to couple a variety of functionalized vinylarenes with alkyl halides applying a nickel-(II) NNN pincer complex in the presence of an NHC-ligated copper catalyst. This combination allows for a 1 mol % loading of the nickel catalyst leading to turnover numbers of up to 72. Over 40 examples are presented, including applications for pharmaceutical diversification. Labeling experiments demonstrated the regioselectivity of the reaction and revealed that the copper catalyst plays a crucial role in enhancing the rate for formation of the reactive linear alkyl nickel complex. Overall, the presented work provides a complimentary approach for hydroalkylation reactions, whilst providing a preliminary mechanistic understanding of the cooperativity between the copper and nickel complexes.

## Introduction

The transition metal catalyzed carbofunctionalization of olefins is a valuable strategy for construction of carbon–carbon bonds, as structurally elaborate saturated compounds can be achieved from an accessible chemical feedstock.<sup>[1]</sup> Although classical coupling strategies evoking alkyl organometallic intermediates have been developed, their reactivity and preparation can be troublesome for couplings with alkyl electrophiles.<sup>[2–6]</sup> To circumvent these challenges, various strategies relying on insertion of the olefin into the transition metal complex have been developed because of the general stability of olefins and the functional group tolerance of this activation approach. Efforts to develop efficient and regioselective functionalization reactions have been made, which have led to advancements for a variety of transformations in hydroarylation/hydroalkenylations,<sup>[7]</sup> hydroalkylations,<sup>[8]</sup> and dicarbofunctionalizations.<sup>[9]</sup> However, difficulty in controlling the regioselectivity without the assistance of a directing group, and challenges associated with undesired  $\beta$ -hydride elimination of the alkyl transition metal complex still persists.

In hydrocarbofunctionalization reactions, a silane is often used as the hydride source for preliminary but mild in situ hydrometalation of olefins. Generally, the regioselectivity of these reductive couplings with respect to the olefin is determined by the hydrometalation step (Scheme 1). However, isomerization via  $\beta$ -hydride elimination between the two regioisomers may occur.<sup>[10,11]</sup> Hydrometalation of unactivated terminal olefins typically leads to linear product formation. Notably, elegant methods using directing groups have enabled access to favor the branched products from terminal alkenes.<sup>[12]</sup> Similarly, metal hydride H-atom transfer (MHAT) strategies have been applied to provide branched selectivity.<sup>[8i,13]</sup> In stark contrast, formation of branched products from activated olefins, such as vinylarenes, are favorably obtained even when using MHAT strategies, and only few examples for the formation of linear products have been reported.<sup>[7g,i,14]</sup>



**Scheme 1.** General approach for the reductive couplings of olefins with an electrophile via hydrometalation.

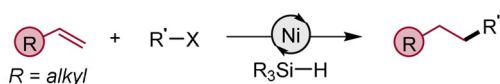
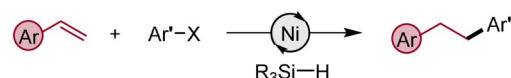
Nickel catalysis has garnered significant interest in the context of hydroalkylation reactions.<sup>[11,15]</sup> Furthermore, as single electron pathways are commonly observed in first row transition metal catalysis, opportunities for the exploitation of alkyl electrophiles as coupling partners has been made possible.<sup>[16–19]</sup> For example, the group of Liu disclosed a hydroalkylation reaction of unactivated terminal olefins with complete linear regioselectivity with a catalyst loading of 10 mol % (Scheme 2).<sup>[8c]</sup> Although this work was broadly applicable to append functionalized fragments, it was limited to only a few examples of primary alkyl halides. Despite significant efforts in Ni-catalyzed hydroalkylation reactions, there are limited examples furnishing linear products from vinylarenes. Lalic and co-workers reported the formation of the linear regioisomer in hydroarylation reaction applying 10 mol % of dichloro(dimethoxyethane)nickel(II) as the precatalyst.<sup>[7j]</sup> Their work describes the use of a variety of olefin coupling partners, but was restricted to aryl halides as the electrophile.

Copper hydride catalysis has been particularly successful for the development of a diverse range of hydrofunctional-

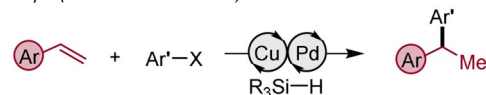
[\*] Dr. A. K. Ravn, Dr. M. B. Johansen, Prof. Dr. T. Skrydstrup  
 Carbon Dioxide Activation Center (CADAC), The Interdisciplinary  
 Nanoscience Center (iNANO) and Department of Chemistry  
 Aarhus University  
 Gustav Wieds Vej 14, 8000 Aarhus (Denmark)  
 E-mail: ts@chem.au.dk

Supporting information and the ORCID identification number(s) for the author(s) of this article can be found under:  
<https://doi.org/10.1002/anie.202112390>.

## Nickel-Catalyzed Hydrofunctionalizations

Csp<sup>3</sup>-Csp<sup>3</sup> (Liu)Csp<sup>2</sup>-Csp<sup>3</sup> (Lalic)

## Dual Cu/Pd-Catalyzed Hydroarylations

Csp<sup>2</sup>-Csp<sup>3</sup> (Nakao & Buchwald)

## Cooperative Cu/Ni-Catalyzed Hydroalkylation

Csp<sup>3</sup>-Csp<sup>3</sup> (This Work)**Scheme 2.** Summary of previous of hydrofunctionalizations and the presented work.

ization reactions. However, its adaptation to coupling with unactivated electrophiles remains challenging.<sup>[20–22]</sup> To enhance the range of such coupling partners, dual catalysis systems were implemented. In 2016, the teams of Nakao and Buchwald independently reported a dual Cu/Pd-catalysis approach for the hydroarylation of vinylarenes (Scheme 2).<sup>[23,24]</sup> These protocols were subsequently expanded to the hydroarylation of unactivated terminal alkenes,<sup>[25]</sup> as well as to hydroalkenylation reactions. Lalic and co-workers recently reported a dual Cu/Ni-catalytic approach for the hydroalkylation of alkynes, however, this work was similarly limited to C(sp<sup>2</sup>)-C(sp<sup>3</sup>) bond formation.<sup>[27]</sup> Additional examples of a beneficial combination of copper complexes in nickel catalysis have been reported in literature.<sup>[28–31]</sup>

Based on these previous reports, we speculated whether the construction of C(sp<sup>3</sup>)-C(sp<sup>3</sup>) bonds may be achieved using Ni-catalysis involving open-shell species via single electron transfer mechanisms in combination with copper hydride catalysis. We expected this approach to potentially expand the scope of hydroalkylation reactions and advance base metal catalysis via a dual catalytic approach. In this work, we disclose our successful efforts to implement such a cooperative system for the linear hydroalkylation of vinylarenes with both primary and secondary alkyl halides. Notably, with a low catalyst loading of only 1 mol % of a simple Ni<sup>II</sup> NNN pincer catalyst, high turnover numbers (TON) are achieved compared to those previously reported. Importantly, the reported methodology attains complete linear regioselectivity, providing a complementary shift from that of the established copper hydride catalysis. Labeling experiments in conjunction with kinetic and empirical studies reveal an essential synergistic effect between the copper and nickel catalysts and, in contrast to previous efforts in combining Cu/Ni-catalysis, the addition of the copper catalyst increases the rate of the hydronicelation step.

## Results and Discussion

Initial studies of this transformation were inspired by the conditions previously reported for the Cu/Pd-catalyzed hydroarylation reactions.<sup>[23,24]</sup> The optimization is detailed in Table 1 using 4-fluorostyrene **1a** as the model substrate and the simple alkyl iodide 3-iodopropylbenzene **2a**. Employing a combination of the Ni<sup>II</sup> NNN pincer complex **C1** in just 1 mol % catalyst loading with *N*-heterocyclic carbene (NHC) ligated Cu<sup>I</sup> catalyst IPrCuCl (5 mol %) provided the linear hydroalkylation product **3a** in 64 % yield (entry 1). The coupling was accomplished using (Me)<sub>2</sub>PhSiH as the hydride source and sodium trimethylsilanolate (TMSNa) as base in THF at 45 °C. Remarkably, the branched hydroalkylation product was not observed. The mass balance of the reaction is approx. 70–80 % with respect to the styrene, and of this some side-product formation was observed as revealed from the spectroscopic analysis of the crude reaction mixture. These products arose from the homocoupling of the alkyl halide, as well as unfruitful reduction pathways, including the direct reduction of both the vinyl group and the alkyl halide.

Excluding the Cu-catalyst afforded only a 5 % yield of the product (entry 2), but resorting to the use of a stoichiometric amount of the NNN pincer Ni<sup>II</sup>-chloride **C1** increased the yield of **3a** to 29 % (entry 3). On the other hand, similar experiments without **C1** with both substoichiometric and

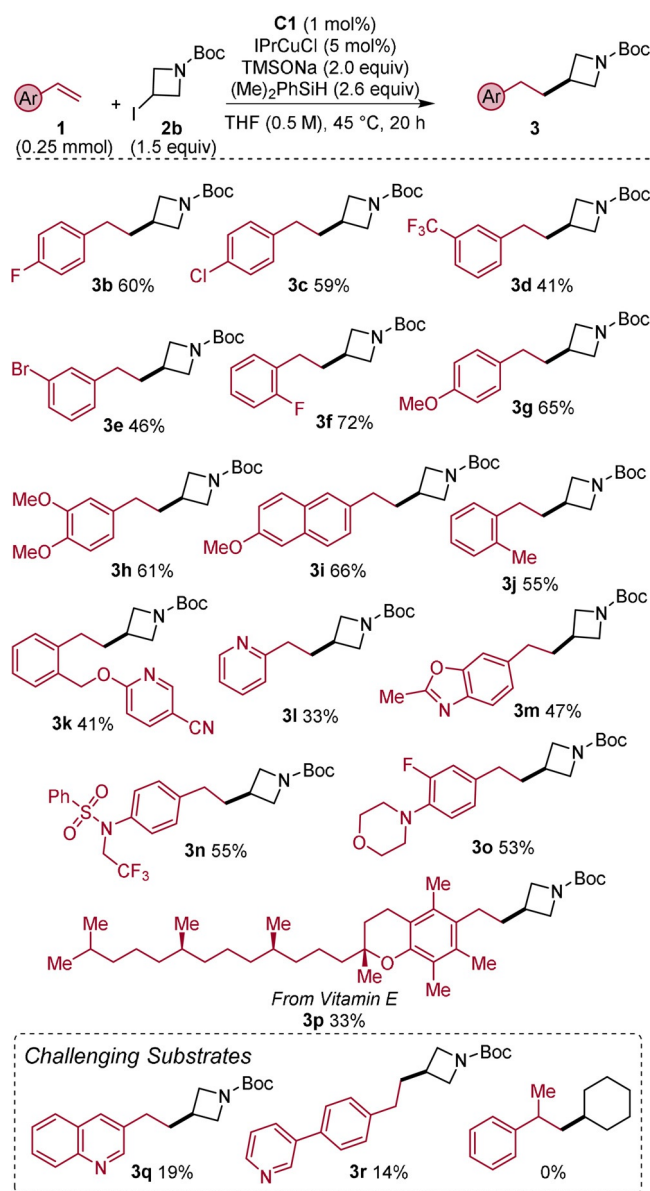
**Table 1:** Optimization of the catalytic hydroalkylation conditions.

	Deviations	Yield <sup>[a]</sup>
1	none	64 %
2	w/o IPrCuCl	5 %
3	<b>C1</b> (1 equiv) w/o IPrCuCl	29 %
4	w/o <b>C1</b>	0 %
5	IPrCuCl (1 equiv) w/o <b>C1</b>	0 %
6	<b>C2</b> i/o <b>C1</b>	6 %
7	NiCl <sub>2</sub> + bipyridine i/o <b>C1</b>	4 %
8	NiCl <sub>2</sub> + terpyridine i/o <b>C1</b>	0 %
9	Ni(COD) <sub>2</sub>	0 %
10	Ni(COD) <sub>2</sub> + <b>L1</b>	28 %
11	SEGPPOS i/o IPr	17 %
12	BINAP i/o IPr	17 %
13	IPrCuCl (2.5 mol %)	55 %
14	0.25 M i/o 0.5 M	56 %
15	35 °C i/o 45 °C	53 %
16	<b>2a</b> (3 equiv)	62 %
17	slow addition (1 h) of <b>2a</b>	34 %
18	<b>2.0 equiv TMSNa</b>	<b>67 %</b>

[a] Yield estimated by <sup>19</sup>F NMR spectroscopy of the crude reaction mixture using fluorobenzene as internal standard. w/o: without, i/o: instead of. IPr: 1,3-Bis(2,6-diisopropylphenyl)imidazol-2-ylidene. COD: 1,5-cyclooctadiene. SEGPPOS: 5,5'-Bis(diphenylphosphino)-4,4'-bi-1,3-benzodioxole. BINAP: 2,2'-Bis(diphenylphosphino)-1,1'-binaphthalene.

stoichiometric amounts of  $\text{IPrCuCl}$  were equally unproductive (entries 4 and 5), indicating the important role of **C1** for the C–C bond forming step. Next, different Ni-catalysts were evaluated (entries 6–8). Surprisingly, the Ni-complex **C2** (nickamine) only afforded a low yield of the desired product. Similarly,  $\text{NiCl}_2$  with bipyridine led to a trace amount of **3a**, whereas no product was observed when employing  $\text{NiCl}_2$  with terpyridine. Using  $\text{Ni}(\text{COD})_2$  did not yield any product formation, however, in combination with the NNN-ligand **L1**, the target product was reached in a 28 % yield (entries 9 and 10). Changing the ligand on the Cu-catalyst from an NHC-ligand to a bidentate phosphine ligand, such as BINAP or SEGPHOS, significantly decreased the yield of the reaction (entries 11 and 12). Furthermore, altering the catalyst loading of  $\text{IPrCuCl}$  from 5 mol % to 2.5 mol % decreased the yield to 55 % (entry 13). Similarly, decreasing the concentration or the reaction temperature gave a lower yield and full consumption of the styrene was not observed (entries 14 and 15). One of the side products formed in this reaction arises from the homocoupling or the reduction of the alkyl iodide. However, no significant change in yield was observed when doubling the amount of the alkyl iodide (entry 16). Additionally, upon slow addition of the alkyl iodide, the yield decreased to 34 % (entry 17). Finally, the amount of base was decreased from four to two equivalents, which eventually provided the optimized conditions, and a yield of 67 % of the coupling product (entry 18). Notable these reaction conditions proceed with a significantly lower loading of the Ni-catalyst (only 1 mol %), and consequently a considerably higher TON, compared to other similar Ni-catalyzed couplings.<sup>[7], [8]</sup>

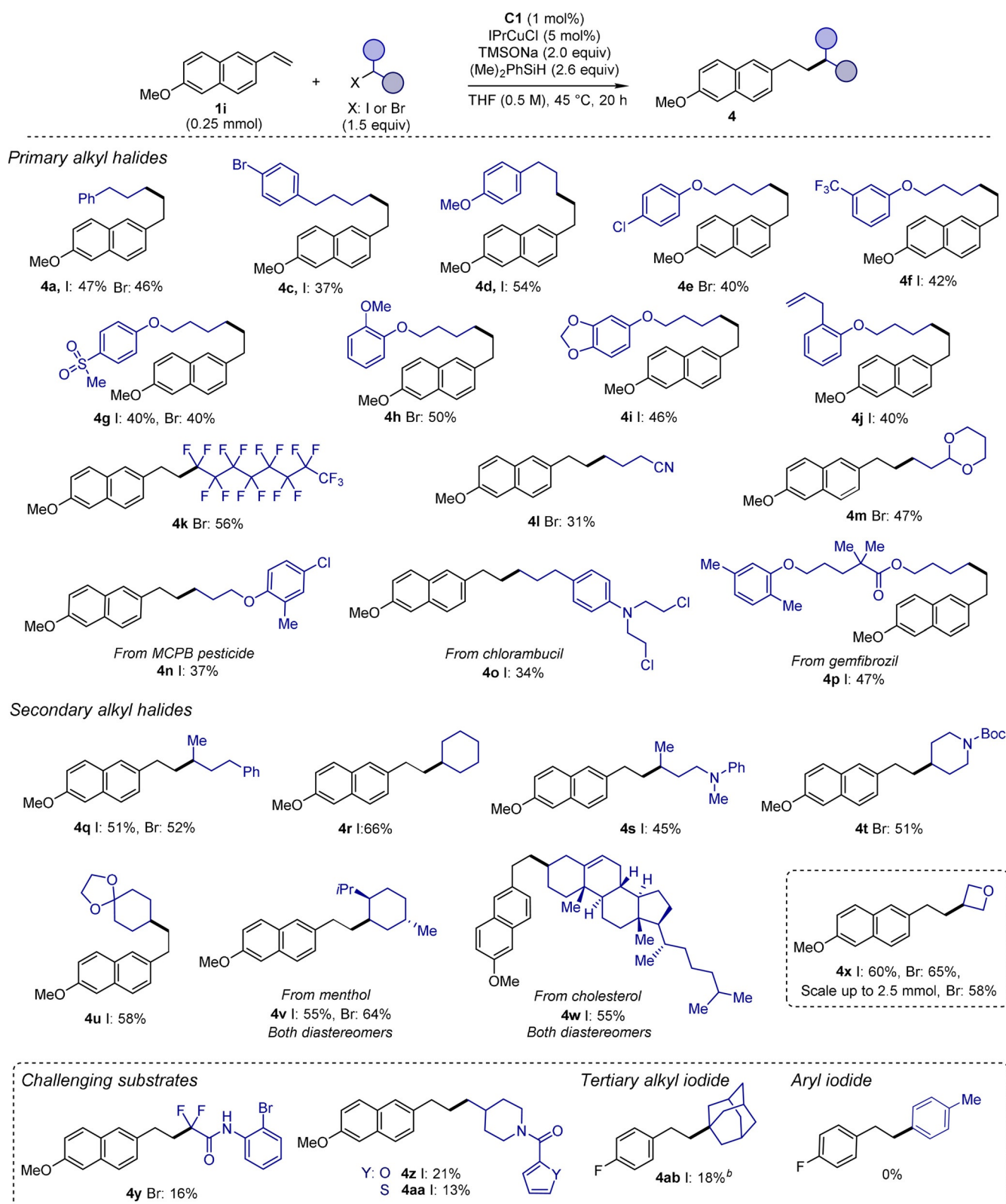
With the optimized conditions in hand, we investigated the generality of this catalytic transformation. For ease of purification due to the apolar nature of the products, we chose *tert*-butyl 3-iodoazetidine-1-carboxylate **2b** as the coupling partner for the scope with varying vinylarenes (Scheme 3). Substrates bearing electron-withdrawing groups on the arene ring in the *para*-, *meta*- or *ortho*-position were converted into the desired products **3b–3f** in moderate to good yields. Notably, both aryl bromides and aryl chlorides were tolerated. Similarly, electron-rich styrene derivatives furnished good yields of the anticipated products **3g–3j**. Next, more functionalized vinylarenes were evaluated. The nicotinonitrile derivative **3k** was obtained in a 41 % yield, while the 2-vinylpyridine afforded the desired product **3l** in 33 % yield. Furthermore, the oxazole-containing product **3m** could be generated and isolated in a 47 % yield. A sulfonamide was tolerated and afforded **3n** in a good yield. Additionally, a morpholine substituted styrene furnished a 53 % yield of the product **3o**. Despite the sterical hindrance by two *ortho*-methyl groups in the vitamin E motif, the desired product **3p** was formed in a decent 33 % yield. The vinylarenes containing quinolines or pyridines proved to be more challenging substrates for this transformation, but nevertheless the anticipated products **3q** and **3r** could be isolated in modest yields. Finally,  $\alpha$ -methylstyrene as a coupling partner was attempted applying these reaction conditions, but the desired product was not obtained.



**Scheme 3.** Substrate scope of vinylarenes. All yields represent the average of the yields isolated product from two reaction runs performed with 0.25 mmol of vinylarene and 1.5 equiv of **2b**. Boc: *tert*-Butyloxycarbonyl. See the Supporting Information for full details.

Next, we investigated the scope of the alkyl halides with 2-methoxy-6-vinylnaphtalene **1i** as the vinylarene substrate (Scheme 4). Primary alkyl halides were first evaluated and both alkyl iodides and bromides were equally amenable for the transformation. This was demonstrated in the synthesis of the simple coupling product **4a**, which was afforded in 47 % yield from the alkyl iodide and 46 % yield from the corresponding bromide. An aryl bromide was tolerated under the reaction conditions providing **4c** in a modest yield. Additionally, the electron-rich methoxy-substituted alkyl iodide yielded a 54 % of **4d**. As earlier seen in Scheme 4, the presence of an aryl chloride in the substrate was not detrimental for product formation, leading to **4e** in a 40 % yield.





**Scheme 4.** Substrate scope of alkyl halides. All yields represent the average of the yields isolated product from two reaction runs performed with 0.25 mmol of vinylarene and 1.5 equiv of **2b**. [b] Yield estimated by  $^1\text{H}$  NMR spectroscopy. See the Supporting Information for full details.

Similar alkyl halides bearing a trifluoromethyl or methyl sulfonyl group on the arene ring could be successfully converted to **4f** and **4g** in approximately 40% yield. The

use of alkyl iodides prepared from guaiacol and sesamol proved equally rewarding leading to the isolation of **4h** and **4i** in a 50% and 46% yield, respectively. Interestingly, an allyl

group was tolerated under these reaction conditions as for **4j** without signs of double bond migration. A perfluorinated alkyl bromide provided **4k** in a good yield and functional groups such as a nitrile and an acetal provided the anticipated products **4l** and **4m** in 31 % and 47 % yield, respectively. Modification of biorelevant structures could also be reached by our methodology. As such, the alkyl iodide derived from the 4-(4-chloro-2-methylphenoxy)butanoic acid (MCPB) pesticide led to formation of **4n** in a 37 % yield and functionalization of the chemotherapeutic drug chlorambucil was accomplished to provide **4o** in a 34 % isolated yield. Furthermore, the pharmaceutically interesting gemfibrozil was converted into the anticipated product **4p** in a 47 % yield. Notably, substrates containing carbonyl groups with enolizable protons are not tolerated under these reaction conditions.

After evaluation of the primary alkyl halides, we turned our attention to the secondary alkyl halides. Again, both secondary alkyl iodides and bromides were equally suitable substrates in the hydroalkylation reaction, which was demonstrated by isolation of the simple product **4q** in a 51 % yield starting from the alkyl iodide, and in a 52 % yield when employing the bromide. Coupling of iodocyclohexane with **1i** was successfully accomplished to afford **4r** in a 66 % yield. An aniline derived secondary alkyl iodide led to the formation of **4s** in a 45 % yield, whereas a Boc-protected piperidine was converted to **4t** in a 51 % yield. Gratifyingly, the presence of a ketal was tolerated under the reaction conditions, providing a 58 % yield of **4u**. Diversification of natural products, such as the menthol motif yielded **4v** in a 55 % yield and in a 64 % yield, employing the iodide and the bromide, respectively. Similarly, without affecting the internal alkene, a derivatized cholesterol was converted to the anticipated product **4w** in a good yield. These two products, **4v** and **4w**, were isolated as a mixture of the two diastereomers, which is consistent with the intermediacy of an open-shell species en route to C(sp<sup>3</sup>)-C(sp<sup>3</sup>) bond formation. Finally, the oxetane-containing product **4x** was prepared in a 60 % yield from the alkyl iodide, and a 65 % yield from the corresponding bromide. The latter was scaled up to 2.5 mmol, which afforded a 58 % yield of the desired product **4x**.

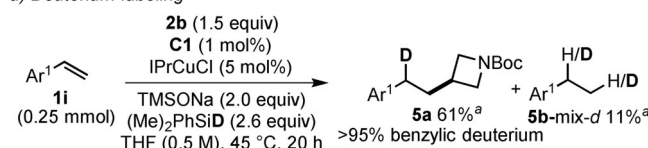
The limitations in electrophilic coupling partner for the transformation were also investigated. The challenging substrate containing a difluoroacetamide was coupled with **1i** to obtain **4y** though in low yield. Similarly, the amide substituted furan and thiophene proved equally challenging for conversion into the desired products, however, **4z** and **4aa** could nonetheless be obtained in 21 % and 13 % yields, respectively. The tertiary alkyl iodide 1-iodoadamantane was subjected to the reaction conditions and afforded the anticipated product **4ab** in an 18 % yield. Generally, for the challenging substrates we still observe some vinylarene after end of reaction. Finally, the coupling of an aryl iodide was attempted, but did not provide the desired product.

We then turned our attention to understanding the mechanistic details of this dual transition metal catalyzed reaction. The regioselectivity of the hydrometalation and the reversibility of this elementary step in the productive pathway was initially investigated with a deuteride source. Performing

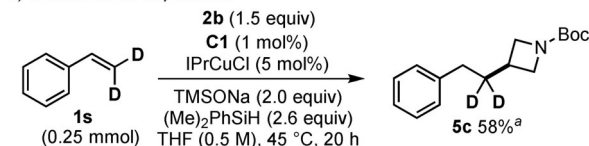
the reaction under the optimized reaction conditions with dimethylphenylsilane-*d* provided the coupling product **5a** bearing a benzylic deuterium (Scheme 5a). This result suggests the formation of a linear hydrometalation complex, which selectively reacts with the alkyl iodide to provide the desired product. The major side-product arising from the vinylarene **1i** is the reduction product **5b**. This side-product was isolated as the reduced vinyl compound **5b-mix-d**, which has deuterium at either or both the benzylic and the terminal position. These side-products can arise from the reduction of either of the regioisomers of the hydrometalation complex. However, as the branched alkylation product is not observed, we speculate that the branched hydrometalation complex may suffer from further reduction, whereas the linear regioisomer selectively reacts with the alkyl halide. To further support this observation, the styrene- $\beta,\beta$ -*d*<sub>2</sub> **1s** was subjected to standard reaction conditions (Scheme 5b). Here, the coupling product **5c** was selectively obtained in a 58 % yield, suggesting that the subsequent C-C bond-forming reaction is substantially faster than  $\beta$ -hydride elimination.

From the initial optimization studies displayed in Table 1, evidence was obtained that for the crucial C-C bond-forming step, the nickel(II) NNN pincer complex **C1** was implicated (Table 1 entries 2–5). As such, this step was studied with a pregenerated Ni-alkyl complex prepared as previously reported from alkyl zinc species.<sup>[32]</sup> Treatment of this organ-

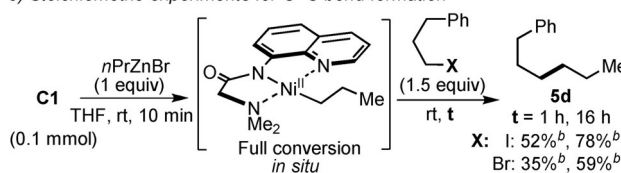
a) Deuterium labeling



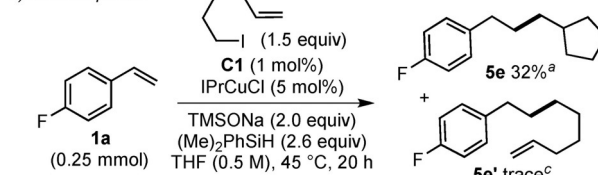
b) Isomerization experiment



c) Stoichiometric experiments for C-C bond formation



d) Radical probe



**Scheme 5.** Mechanistic investigations of the dual metal catalytic system. [a] Yield of isolated product. [b] Yield estimated by <sup>1</sup>H NMR spectroscopy using 1,3,5-trimethoxybenzene as internal standard. [c] Detected by <sup>1</sup>H NMR spectroscopy. See the Supporting Information for full details of the above reactions.

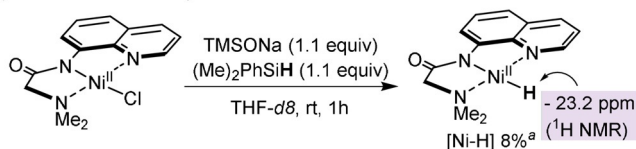
ometallic complex with either an alkyl iodide or bromide for 1 h provided the desired product **5d** in a 52% or 35% yield, respectively. Increasing the reaction time afforded an increase in the yields to 78% or 59%, respectively (Scheme 5c). A bimetallic oxidative addition pathway involving intermediate carbon-centered radicals was proposed in previous studies for these coupling reactions.<sup>[32–34]</sup> Hence, similar to this earlier work, a radical probe experiment using 6-iodohex-1-ene equally revealed the generation of alkyl radical intermediates affording the ring-closed product **5e** in a 32% yield and trace amounts of the linear product **5e'** (Scheme 5d). Based on these experiments, the C(sp<sup>3</sup>)–C(sp<sup>3</sup>) bond formation is suggested to proceed by addition of the reactive open-shell species to a Ni<sup>II</sup>-alkyl complex followed by an ensuing and rapid reductive elimination.

We were interested in further understanding the hydrometalation step in the reaction, as the regioselectivity observed in this work represented a shift from the well-established copper hydride catalysis. As such, we performed stoichiometric experiments to investigate whether nickel was the active metal-hydride species (Scheme 6). Treatment of **C1** with dimethylphenylsilane in combination with TMSNa at ambient temperature provided a hydride species in 8% yield as determined by a singlet present at –23.2 ppm in the <sup>1</sup>H NMR spectrum (Scheme 6a), which is comparable with literature reports of a similar NNN pincer Ni<sup>II</sup> hydride complex (**C2** hydride).<sup>[35]</sup> Furthermore, nickel hydride formation in hydroamination reactions with a directing group corresponding to our ligand backbone has been demonstrated.<sup>[36]</sup> Additionally, when using the deuteride source, dimethylphenylsilane-*d*, the singlet peak for the hydride was not observed (see the Supporting Information (SI)). Nevertheless, several attempts to isolate the nickel hydride species

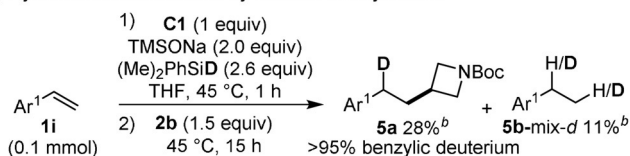
generated from **C1** were unsuccessful, which can possibly be accounted for by its low chemical stability as previously suggested from other studies.<sup>[35,37]</sup> With this finding in hand, we subjected 2-methoxy-6-vinylnaphthalene **1i** to the stoichiometric conditions for nickel hydride formation in an attempt to form the reactive Ni-alkyl complex. Subsequent addition of the *N*-Boc-2-iodoazetidine **2b** to the reaction mixture provided a 28% yield of the anticipated product **5a** bearing deuterium at the benzylic position, which is in correlation with the catalytic experiment in Scheme 5a. Furthermore, the reduced vinylarene **5b** was observed as the major side-product along with remaining unreacted vinylarene **1i**. The reduced side-products **5b-mix-d** is a mixture of deuterium labeled ethylarenes. These stoichiometric experiments support the hypothesis that only the linear hydronickelation complex reacts with the alkyl halide. Although the nickel complex can form the desired product without copper, the addition of copper increases the yield of the reaction, and the TON of the nickel catalyst (Table 1, entries 2–5). To elucidate whether copper was involved in stabilizing the linear hydronickelation complex via transmetalation, the in situ formed Ni-alkyl complex was studied in the presence of the IPrCuCl complex (Scheme 6c). However, no reaction between the two complexes was observed.

To elucidate the role of copper in the transformation, we performed additional stoichiometric experiments for the hydrometalation step with the copper complex (Scheme 7). Hydrocupration of 2-methoxy-6-vinylnaphthalene **1i** with IPrCuCl using dimethylphenylsilane-*d* afforded selectively the reduced product **5b-β-d'** with deuterium placed at the terminal position upon work up, being in agreement with literature reports (Scheme 7a).<sup>[23]</sup> This was further demonstrated by the hydrocupration of 4-fluorostyrene **1a** to form the branched complex **6a**.<sup>[23,38]</sup> Although the regioselectivity of hydrocupration did not correlate with the product observed in this work, the complex **6a** could not initially be excluded as part of the productive pathway for product formation. To

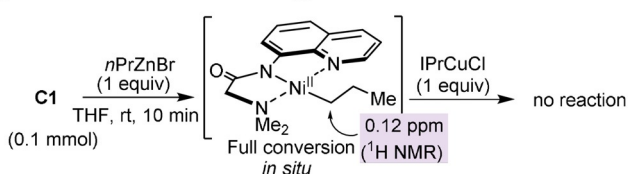
a) Detection of nickel hydride



b) Hydronickelation followed by addition of alkyl iodide

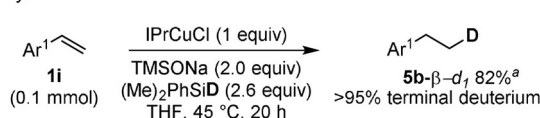


c) Transmetalation from nickel to copper

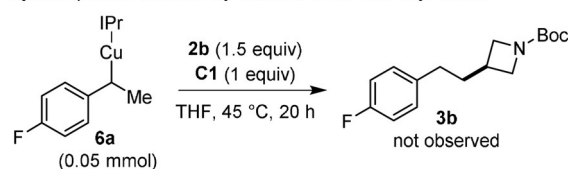


**Scheme 6.** Stoichiometric hydrometalation experiments with nickel complexes. [a] Yield estimated by <sup>1</sup>H NMR spectroscopy using 1,3,5-trimethoxybenzene as internal standard. [b] Yield of the isolated product. See the Supporting Information for full details of the above reactions.

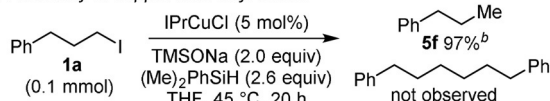
a) Hydrometalation with IPrCuCl



b) Hydrocupration followed by addition of C1 and alkyl iodide



c) Reactivity of copper with alkyl iodide



**Scheme 7.** Stoichiometric hydrometalation experiments with copper. [a] Yield of the isolated product. [b] Yield estimated by <sup>1</sup>H NMR spectroscopy using 1,3,5-trimethoxybenzene as internal standard. See Supporting Information for full details of the above reactions.



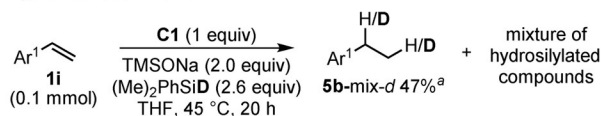
investigate the importance of complex **6a**, it was subsequently treated with the alkyl iodide **2b** and stoichiometric amounts of the Ni-complex **C1**. However, the product **3b** was not observed (Scheme 7b). Subjecting complex **6a** to stoichiometric amounts of **C1** leads to some degradation to the reduced vinylarene and styrene, whilst no transmetalation is observed between these two species as monitored by  $^1\text{H}$  and  $^{19}\text{F}$  NMR spectroscopy (see SI). Finally, we investigated the reactivity of the copper complex with the alkyl iodide to elucidate whether copper plays a role in the formation of the carbon-centered radical (Scheme 7c). However, the homo-coupling of the alkyl iodide was not observed and the reaction afforded a 97% yield of the corresponding alkane **5f**. Further studies on the reactivity between copper and the alkyl halide did not indicate formation of alkyl radical (see SI).

Further investigations of the hydrometalation step with both catalysts were performed. Interestingly, hydronicelation of **1i** using dimethylphenylsilane-*d* provided a mixture of deuterium labeled reduced vinylarenes **5b-mix-d** in a 47% yield and a mixture of hydrosilylated products from **1i** (Scheme 8a). Next, we subjected **1i** to both **C1** and IPrCuCl under hydrometalation conditions (Scheme 8b). The yield of **5b-mix-d** increased to 63% and the linear hydrosilylated products **5g-mix-d** were isolated in a 14% yield. The hydrosilylation of **1i** was refuted as an intermediate, as the desired alkylated product was not observed when subjecting **5g** to the reaction conditions (see SI). Interestingly, following the hydrometalation experiments over time elucidated the effect of copper (Scheme 8c). The reaction mixture was heated to

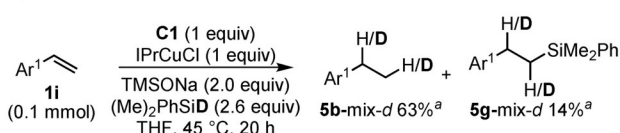
45°C for 5 min before being analyzed by  $^2\text{H}$  NMR, and the estimated yield of deuterium at the benzylic position was followed over time. Although the IPrCuCl favors the branched regioisomer in the hydrometalation step giving rise to deuterium at the terminal position (Scheme 7a), the addition of copper enhanced the rate of incorporation of deuterium at the benzylic position. Notably, the overall rate of the reduction reaction was increased significantly upon addition of copper. Based on these findings, we reasoned that copper increases the rate for the formation of the linear Ni-alkyl complex. We speculate that this occurs by copper increasing the rate of nickel hydride formation. Additional stoichiometric experiments were performed to elucidate whether a transmetalation from copper hydride to the NNN pincer  $\text{Ni}^{\text{II}}$ -chloride was reasonable. However, these experiments did not indicate that the transmetalation provided a more efficient formation of the nickel hydride (see SI).

A mechanistic proposal is outlined in Scheme 9. The catalytic cycle is based upon our studies and literature on

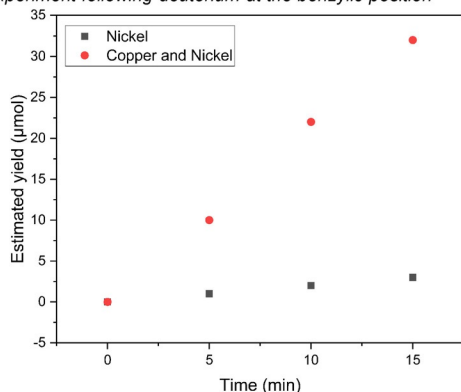
a) Hydrometalation with **C1**



b) Hydrometalation with IPrCuCl and **C1**

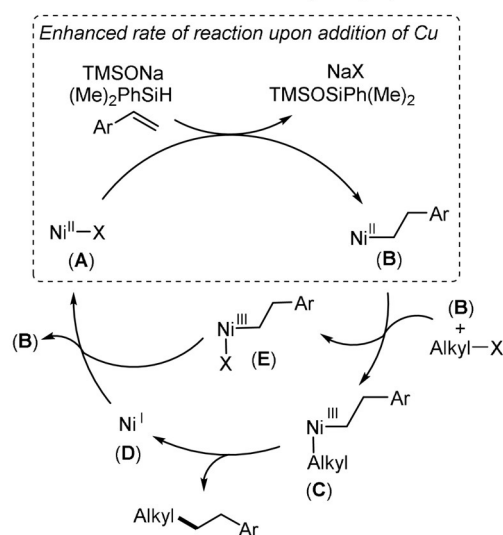


c) Time experiment following deuterium at the benzylic position

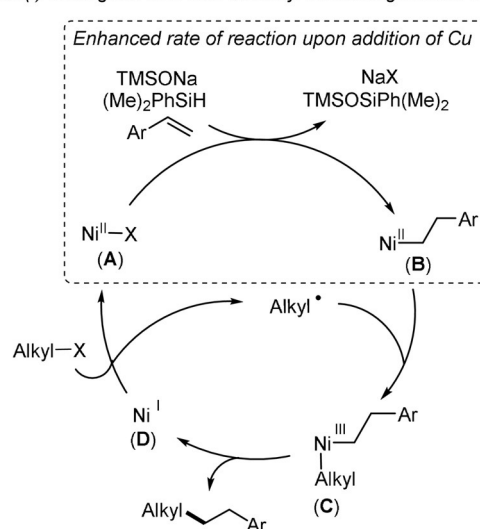


**Scheme 8.** Hydrometalation experiments with **1i** for understanding the role of copper. [a] Yield of isolated product. See Supporting Information for full details of the above reactions.

a) Bimetallic oxidative addition followed by comproportionation



b)  $\text{Ni}(\text{I})$  undergoes SET with the alkyl halide to generate the alkyl radical



**Scheme 9.** Proposal of possible catalytic cycles.

similar nickel catalyzed hydroalkylation reaction mechanisms.<sup>[15]</sup> From our stoichiometric studies of the hydrometalation step, we propose that hydronickelation of the vinylarene provides the Ni-alkyl complex **B**. Furthermore, we suggest that the Cu-complex enhances the rate of the formation of **B**. These findings indicate that the turnover limiting step for the catalysis is represented by the conversion of the nickel complex **A** into the linear nickel alkyl species **B**. We propose that complex **B** selectively reacts with the alkyl halide, as the benzylic deuterium label is exclusively observed in the product. A bimetallic oxidative addition pathway with the alkyl halide may then take place providing two distinct Ni<sup>III</sup> complexes (Scheme 8a). This mechanism is in line with the extensive mechanistic investigation by Hu and co-workers on the cross-coupling of alkyl halides with organomagnesium reagents catalyzed by the Ni<sup>II</sup> NN<sub>2</sub> pincer complex, nickelamine.<sup>[33,34]</sup> Inner sphere single electron transfer (SET) from **B** forms a Ni<sup>III</sup>-(alkyl)halide complex **E** and a carbon-centered radical, which recombines with a second Ni<sup>II</sup>-alkyl complex **B** to produce the Ni<sup>III</sup> species **C**. Rapid reductive elimination releases the product and the Ni<sup>I</sup>-species **D**. Finally, comproportionation between complexes **E** and **D** leads to the formation of the Ni<sup>II</sup>-alkyl complex **B**, which can re-enter the catalytic cycle, as well as the re-generation of the Ni<sup>II</sup>-halide complex **A**.

An alternative pathway for the formation of the carbon-centered radical may be considered under the catalytic conditions as well, as illustrated by the catalytic cycle in Scheme 9b. We have previously proposed an inner sphere electron transfer pathway involving the Ni<sup>I</sup> NNN pincer complex **D** and the alkyl halide in our work on the carbon-ylation coupling of alkyl iodides with organozinc reagents.<sup>[39]</sup> Subsequently, combining the carbon-centered radical with the Ni complex **B** formed from the hydrometalation step leads to the high-valent Ni species **C**. To finish the cycle, reductive elimination provides the product and Ni<sup>I</sup>. There is the possibility that both catalytic cycles could be operating under these reaction conditions.

## Conclusion

In summary, we have realized the hydroalkylation of vinylarenes with complete linear regioselectivity through the exploitation of a dual catalytic system involving both copper and nickel. Importantly, these observations are in contrast with earlier studies involving copper hydride catalysis whereby branched selectivity is favored. Over 40 examples were demonstrated applying the developed chemistry for carbon-(sp<sup>3</sup>)-carbon(sp<sup>3</sup>) bonds between an alkyl halide and a vinylarene, and the methodology was also applicable to the diversification of pharmaceutically relevant compounds. Pleasingly, the Ni<sup>II</sup> NNN pincer catalyst functioned well, even with a catalyst loading of only 1 mol%, which gives TONs up to 72 for the nickel catalyst. In our mechanistic investigations of this interesting coupling reaction, insight into the essential synergistic effect between the copper and nickel catalysts was provided. Labeling studies of the hydrometalation step demonstrate the complete regioselectivity of

the transformations. Although the hydrometalation may not be completely selective, the subsequent C–C bond-forming step only occurs with the intermediate formed from linear hydronickelation. Moreover, a radical probe experiment provides evidence for an intermediate carbon-centered radical in the productive pathway to C–C bond formation. Stoichiometric experiments with the two catalysts indicate that addition of copper increases the rate for formation of the reactive linear alkyl nickel complex. We anticipate that the presented approach can provide an additional but significant avenue in mild hydroalkylation reactions.

## Acknowledgements

We are highly appreciative of financial support from the Danish National Research Foundation (grant no. DNR118), the Independent Research Fund Denmark—Technology and Production (grant no. 4148-00031), and Aarhus University for financial support.

## Conflict of Interest

The authors declare no conflict of interest.

**Keywords:** dual catalysis · hydroalkylation · metal hydrides · regioselectivity · vinylarenes

- [1] For selected reviews, see: a) Y. Yamamoto, U. Radhakrishnan, *Chem. Soc. Rev.* **1999**, 28, 199–207; b) R. I. McDonald, G. Liu, S. S. Stahl, *Chem. Rev.* **2011**, 111, 2981–3019; c) P. Gandeepan, C. H. Cheng, *Acc. Chem. Res.* **2015**, 48, 1194–1206; d) E. A. Standley, S. Z. Tasker, K. L. Jensen, T. F. Jamison, *Acc. Chem. Res.* **2015**, 48, 1503–1514; e) S. W. M. Crossley, C. Obradors, R. M. Martinez, R. A. Shenvi, *Chem. Rev.* **2016**, 116, 8912–9000; f) J. C. Lo, D. Kim, C.-M. Pan, J. T. Edwards, Y. Yabe, J. Gui, T. Qin, S. Gutierrez, J. Giacoboni, M. W. Smith, P. L. Holland, P. S. Baran, *J. Am. Chem. Soc.* **2017**, 139, 2484–2503; g) Z. Dong, Z. Ren, S. J. Thompson, Y. Xu, G. Dong, *Chem. Rev.* **2017**, 117, 9333–9403; h) L. J. Oxtoby, J. A. Gurak, S. R. Wisniewski, M. D. Eastgate, K. M. Engle, *Trends Chem.* **2019**, 1, 572–587; i) J. Diccianni, Q. Lin, T. Diao, *Acc. Chem. Res.* **2020**, 53, 906–919.
- [2] M. R. Netherton, G. C. Fu, *Adv. Synth. Catal.* **2004**, 346, 1525–1532.
- [3] A. C. Frisch, M. Beller, *Angew. Chem. Int. Ed.* **2005**, 44, 674–688; *Angew. Chem.* **2005**, 117, 680–695.
- [4] A. Rudolph, M. Lautens, *Angew. Chem. Int. Ed.* **2009**, 48, 2656–2670; *Angew. Chem.* **2009**, 121, 2694–2708.
- [5] R. Jana, T. P. Pathak, M. S. Sigman, *Chem. Rev.* **2011**, 111, 1417–1492.
- [6] J. Choi, G. Fu, *Science* **2017**, 356, eaaf7230.
- [7] For selected examples of hydroarylations with aryl halides, see: a) G. C. Tsui, M. Lautens, *Angew. Chem. Int. Ed.* **2010**, 49, 8938–8941; *Angew. Chem.* **2010**, 122, 9122–9125; b) G. C. Tsui, F. Menard, M. Lautens, *Org. Lett.* **2010**, 12, 2456–2459; c) S. A. Green, J. L. M. Matos, A. Yagi, R. A. Shenvi, *J. Am. Chem. Soc.* **2016**, 138, 12779–12782; d) F. Chen, K. Chen, Y. Zhang, Y. He, Y.-M. Wang, S. Zhu, *J. Am. Chem. Soc.* **2017**, 139, 13929–13935; e) M. L. O'Duill, R. Matsuura, Y. Wang, J. L. Turnbull, J. A. Gurak, Jr., D.-W. Gao, G. Lu, P. Liu, K. M. Engle, *J. Am. Chem. Soc.* **2017**, 139, 15576–15579; f) H. Wang, Z. Bai, T. Jiao, Z.



- Deng, H. Tong, G. He, Q. Peng, G. Chen, *J. Am. Chem. Soc.* **2018**, *140*, 3542–3546; g) L. Jin, J. Qian, N. Sun, B. Hu, Z. Shen, X. Hu, *Chem. Commun.* **2018**, *54*, 5752–5755; h) C. Wang, G. Xiao, T. Guo, Y. Ding, X. Wu, T.-P. Loh, *J. Am. Chem. Soc.* **2018**, *140*, 9332–9336; i) S. A. Green, S. Vázquez-Céspedes, R. A. Shenvi, *J. Am. Chem. Soc.* **2018**, *140*, 11317–11324; j) A. J. Gurak, Jr., K. M. Engle, *ACS Catal.* **2018**, *8*, 8987–8992; k) R. Matsuura, T. C. Jenkins, D. E. Hill, K. S. Yang, G. M. Gallego, S. Yang, M. He, F. Wang, R. P. Marsters, I. McAlpine, K. M. Engle, *Chem. Sci.* **2018**, *9*, 8363–8368; l) J. Nguyen, A. Chong, G. Lalic, *Chem. Sci.* **2019**, *10*, 3231–3236; m) D.-M. Wang, W. Feng, Y. Wu, T. Liu, P. Wang, *Angew. Chem. Int. Ed.* **2020**, *59*, 20399–20404; *Angew. Chem.* **2020**, *132*, 20579–20584.
- [8] For selected examples of hydroalkylations with alkyl halides see: a) R. M. Maksymowicz, P. M. C. Roth, S. P. Fletcher, *Nat. Chem.* **2012**, *4*, 649–654; b) Y. M. Wang, N. C. Bruno, Á. L. Placeres, S. Zhu, S. L. Buchwald, *J. Am. Chem. Soc.* **2015**, *137*, 10524–10527; c) X. Lu, B. Xiao, Z. Zhang, T. Gong, W. Su, J. Yi, Y. Fu, L. Liu, *Nat. Commun.* **2016**, *7*, 11129; d) Z. Wang, H. Yin, G. C. Fu, *Nature* **2018**, *563*, 379–383; e) F. Zhou, J. Zhu, Y. Zhang, S. Zhu, *Angew. Chem. Int. Ed.* **2018**, *57*, 4058–4062; *Angew. Chem.* **2018**, *130*, 4122–4126; f) F. Zhou, Y. Zhang, X. Xu, S. Zhu, *Angew. Chem. Int. Ed.* **2019**, *58*, 1754–1758; *Angew. Chem.* **2019**, *131*, 1768–1772; g) H. Pang, Y. Wang, F. Gallou, B. H. Lipshutz, *J. Am. Chem. Soc.* **2019**, *141*, 17117–17124; h) S. Bera, X. Hu, *Angew. Chem. Int. Ed.* **2019**, *58*, 13854–13859; *Angew. Chem.* **2019**, *131*, 13992–13997; i) S.-Z. Sun, C. Romano, R. Martin, *J. Am. Chem. Soc.* **2019**, *141*, 16197–16201; j) S. A. Green, T. R. Huffman, R. O. McCourt, V. van der Puyl, R. A. Shenvi, *J. Am. Chem. Soc.* **2019**, *141*, 7709–7714; k) S.-J. He, J.-W. Wang, Y. Li, Z.-Y. Xu, X.-X. Wang, X. Lu, Y. Fu, *J. Am. Chem. Soc.* **2020**, *142*, 214–221; l) Z.-P. Yang, G. C. Fu, *J. Am. Chem. Soc.* **2020**, *142*, 5870–5875; m) S. Bera, R. Mao, X. Hu, *Nat. Chem.* **2021**, *13*, 270–277; n) J.-W. Wang, Y. Li, W. Nie, Z. Chang, Z.-A. Yu, Y.-F. Zhao, X. Lu, Y. Fu, *Nat. Commun.* **2021**, *12*, 1313; o) X.-X. Wang, L. Yu, X. Lu, Z.-L. Zhang, D.-G. Liu, C. Tian, Y. Fu, *CCS Chem.* **2021**, *3*, 727–737.
- [9] For selected examples of dicarbofunctionalizations see: a) A. García-Domínguez, Z. Li, C. Nevado, *J. Am. Chem. Soc.* **2017**, *139*, 6835–6838; b) W. Shu, A. García-Domínguez, M. T. Quirós, R. Mondal, D. J. Cárdenas, C. Nevado, *J. Am. Chem. Soc.* **2019**, *141*, 13812–13821; c) X. Wei, W. Shu, A. García-Domínguez, E. Merino, C. Nevado, *J. Am. Chem. Soc.* **2020**, *142*, 13515–13522; d) Y. C. Luo, C. Xu, X. Zhang, *Chin. J. Chem.* **2020**, *38*, 1371–1394; e) J. Derosa, O. Apolinar, T. Kang, V. T. Tran, K. M. Engle, *Chem. Sci.* **2020**, *11*, 4287–4296.
- [10] E. Larionov, H. Li, C. Mazet, *Chem. Commun.* **2014**, *50*, 9816–9826.
- [11] A. Vasseur, J. Bruffaerts, I. Marek, *Nat. Chem.* **2016**, *8*, 209–219.
- [12] Z.-Q. Li, O. Apolinar, R. Deng, K. M. Engle, *Chem. Sci.* **2021**, *12*, 11038–11044.
- [13] S. A. Green, S. W. M. Crossley, J. L. M. Matos, S. Vázquez-Céspedes, S. L. Shevick, R. A. Shenvi, *Acc. Chem. Res.* **2018**, *51*, 2628–2640.
- [14] T. Sigeru, T. Hideo, M. Kazuo, *Chem. Lett.* **1985**, *14*, 1353–1354.
- [15] X.-X. Wang, X. Lu, Y. Li, J.-W. Wang, Y. Fu, *Sci. China Chem.* **2020**, *63*, 1586–1600.
- [16] X. Hu, *Chem. Sci.* **2011**, *2*, 1867–1886.
- [17] S. Z. Tasker, E. A. Standley, T. F. Jamison, *Nature* **2014**, *509*, 299–309.
- [18] V. P. Ananikov, *ACS Catal.* **2015**, *5*, 1964–1971.
- [19] J. B. Dicciani, T. Diao, *Trends Chem.* **2019**, *1*, 830–844.
- [20] C. Deutsch, N. Krause, B. H. Lipshutz, *Chem. Rev.* **2008**, *108*, 2916–2927.
- [21] M. T. Pirnot, Y. M. Wang, S. L. Buchwald, *Angew. Chem. Int. Ed.* **2016**, *55*, 48–57; *Angew. Chem.* **2016**, *128*, 48–57.
- [22] R. Y. Liu, S. L. Buchwald, *Acc. Chem. Res.* **2020**, *53*, 1229–1243.
- [23] K. Semba, K. Ariyama, H. Zheng, R. Kameyama, S. Sakaki, Y. Nakao, *Angew. Chem. Int. Ed.* **2016**, *55*, 6275–6279; *Angew. Chem.* **2016**, *128*, 6383–6387.
- [24] S. D. Friis, M. T. Pirnot, S. L. Buchwald, *J. Am. Chem. Soc.* **2016**, *138*, 8372–8375.
- [25] S. D. Friis, M. T. Pirnot, L. N. Dupuis, S. L. Buchwald, *Angew. Chem. Int. Ed.* **2017**, *56*, 7242–7246; *Angew. Chem.* **2017**, *129*, 7348–7352.
- [26] A. W. Schuppe, J. V. Knippel, G. M. Borrajo-Calleja, S. L. Buchwald, *J. Am. Chem. Soc.* **2021**, *143*, 5330–5335.
- [27] A. Hazra, J. Chen, G. Lalic, *J. Am. Chem. Soc.* **2019**, *141*, 12464–12469.
- [28] K. Semba, Y. Ohtagaki, Y. Nakao, *Org. Lett.* **2016**, *18*, 3956–3959.
- [29] a) C. Zarate, R. Martin, *J. Am. Chem. Soc.* **2014**, *136*, 2236–2239; b) R. J. Somerville, L. V. A. Hale, E. Gómez-Bengoia, J. Burés, R. Martin, *J. Am. Chem. Soc.* **2018**, *140*, 8771–8780.
- [30] P. Basnet, S. K. C. R. K. Dhungana, B. Shrestha, T. J. Boyle, R. Giri, *J. Am. Chem. Soc.* **2018**, *140*, 15586–15590.
- [31] J. Xia, T. Hirai, S. Katayama, H. Nagae, W. Zhang, K. Mashima, *ACS Catal.* **2021**, *11*, 6643–6655.
- [32] T. L. Andersen, A. S. Donslund, K. T. Neumann, T. Skrydstrup, *Angew. Chem. Int. Ed.* **2018**, *57*, 800–804; *Angew. Chem.* **2018**, *130*, 808–812.
- [33] J. Breitenfeld, J. Ruiz, M. D. Wodrich, X. Hu, *J. Am. Chem. Soc.* **2013**, *135*, 12004–12012.
- [34] J. Breitenfeld, M. D. Wodrich, X. Hu, *Organometallics* **2014**, *33*, 5708–5715.
- [35] J. Breitenfeld, R. Scopelliti, X. Hu, *Organometallics* **2012**, *31*, 2128–2136.
- [36] J. Jeon, C. Lee, H. Seo, S. Hong, *J. Am. Chem. Soc.* **2020**, *142*, 20470–20480.
- [37] S. J. Ton, K. T. Neumann, P. Nørby, T. Skrydstrup, *J. Am. Chem. Soc.* **2021**, *143*, 17816–17824.
- [38] Y. Xi, J. F. Hartwig, *J. Am. Chem. Soc.* **2017**, *139*, 12758–12772.
- [39] A. S. Donslund, S. S. Pedersen, C. Gaardbo, K. T. Neumann, L. Kingston, C. S. Elmore, T. Skrydstrup, *Angew. Chem. Int. Ed.* **2020**, *59*, 8099–8103; *Angew. Chem.* **2020**, *132*, 8176–8180.

Manuscript received: September 12, 2021

Revised manuscript received: October 14, 2021

Accepted manuscript online: November 2, 2021

Version of record online: December 9, 2021